Application of the Extended Clearance Classification System (ECCS) in Drug Discovery and Development: Selection of Appropriate In Vitro Tools and Clearance Prediction [S]

Kenichi Umehara, Carina Cantrill, Matthias Beat Wittwer, Elisa Di Lenarda, Florian Klammers, Aynur Ekiciler, Neil Parrott, ⓘStephen Fowler, and Mohammed Ullah

Pharmaceutical Sciences, Roche Pharmaceutical Research and Early Development, Roche Innovation Center, Basel, Switzerland

ABSTRACT

In vitro to in vivo extrapolation (IVIVE) to predict human hepatic clearance, including metabolism and transport, requires extensive experimental resources. In addition, there may be technical challenges to measure low clearance values. Therefore, prospective identification of rate-determining step(s) in hepatic clearance through application of the Extended Clearance Classification System (ECCS) could be beneficial for optimal compound characterization. IVIVE for hepatic intrinsic clearance (CLint,h) prediction is conducted for a set of 36 marketed drugs with low-to-high in vivo clearance, which are substrates of metabolic enzymes and active uptake transporters in the liver. The compounds were assigned to the ECCS classes, and CLint,h, estimated with HepatoPac (a micropatterned hepatocyte coculture system), was compared with values calculated based on suspended hepatocyte incubates. An apparent permeability threshold (apical to basal) of 50 nm/s in LLC-PK1 cells proved optimal for ECCS classification. A reasonable performance of the IVIVE for compounds across multiple classes using HepatoPac was achieved (with 2–3-fold error), except for substrates of uptake transporters (class 3b), for which scaling of uptake clearance using plated hepatocytes is more appropriate. Irrespective of the ECCS assignment, metabolic clearance can be estimated well using HepatoPac. The validation and approach elaborated in the present study can result in proposed decision trees for the selection of the optimal in vitro assays guided by ECCS class assignment, to support compound optimization and candidate selection.

SIGNIFICANCE STATEMENT

Characterization of the rate-determining step(s) in hepatic elimination could be on the critical path of compound optimization during drug discovery. This study demonstrated that HepatoPac and plated hepatocytes are suitable tools for the estimation of metabolic and active uptake clearance, respectively, for a larger set of marketed drugs, supporting a comprehensive strategy to select optimal in vitro tools and to achieve Extended Clearance Classification System–dependent in vitro to in vivo extrapolation for human clearance prediction.

Introduction

Most drugs are eliminated from systemic circulation by pathways involving the kidney or liver. Hepatic elimination is the net result of drug uptake over the sinusoidal membrane (carrier- and non–carrier-mediated), followed by metabolism and/or biliary excretion, with some cases in which drugs can also undergo passive escape from the hepatocytes back to the systemic circulation (Kusuhara and Sugiyama, 2010). These individual clearance processes can be measured in conventional systems such as primary hepatocytes, liver microsomes, and sandwich-cultured hepatocytes (Iwatsubo et al., 1997; Swift et al., 2010; Watanabe et al., 2010). However, in vitro to in vivo extrapolation (IVIVE) to predict hepatic clearance (CLh) requires significant experimental resources (Camenisch and Umehara, 2012), and since metabolically stable compounds are preferred as drug candidates due to their longer retention in the body (Murgasova, 2019), reliable measurements of low metabolic clearance values can be a bottleneck. Furthermore, metabolically stable compounds are more likely to undergo hepatobiliary transport, warranting consideration of additional pathways to avoid mispredictions in hepatic intrinsic clearance (CLint,h). Accordingly, a holistic approach for the prediction of CLint,h has been demonstrated using the Extended Clearance Model, which integrates the major hepatic clearance processes: influx clearance (PSinf = PSinf,passive + PSinf,active) for

ABBREVIATIONS: BCRP, breast cancer resistance protein; CLh, hepatic clearance; CLh,b, hepatic blood clearance; CLh,p, hepatic plasma clearance; CLint,h, hepatic intrinsic clearance; CLmet, metabolic clearance; CLothers, other pathway clearance; CLr,p, renal plasma clearance; CLtot,p, total plasma clearance; ECCS, Extended Clearance Classification System; FCS, fetal calf serum; fu,b, unbound fraction in blood; fu,p, unbound fraction in plasma; fu(inc), unbound fraction in incubates; HBSS, Hanks' balanced salt solution; IVIVE, in vitro to in vivo extrapolation; LC-MS/MS, liquid chromatography–tandem mass spectrometry; LLC-PK1, Lilly Laboratories Cell Porcine Kidney 1; MW, molecular weight; OAT, organic anion transporter; OATP, organic anion transporting polypeptide; OCT, organic cation transporter; Papp, apparent permeability; P-gp, P-glycoprotein; PK, pharmacokinetic; PSbile, biliary excretion clearance; PSeff, back-flux clearance; PSinf, influx clearance; Rb, blood-to-plasma concentration ratio; UGT, UDP-glucuronosyltransferase.

uptake, metabolic clearance (CLmet) for metabolism, PSbile for biliary excretion, and PSeff for backflux (Camenisch and Umehara, 2012; Umehara and Camenisch, 2012).

Characterization of the rate-determining step(s) in hepatic elimination could be on the critical path during drug discovery, since this could direct optimization toward the most relevant in vitro parameters for a given drug candidate series. The framework of an Extended Clearance Classification System (ECCS) has been proposed and was verified using 307 compounds with a single clearance mechanism contributing to ≥70% of systemic clearance (Varma et al., 2015): class 1a [hepatic metabolism; molecular weight (MW) ≤400, acids/zwitterions, and high permeability], class 1b (hepatic uptake; MW >400, acids/zwitterions, and high permeability), class 2 (hepatic metabolism; bases/neutrals and high permeability), class 3a (renal elimination; MW ≤400, acids/zwitterions, and low permeability), class 3b (hepatic uptake and/or renal elimination; MW >400, acids/zwitterions, and low permeability), and class 4 (renal elimination; bases/neutrals and low permeability). Of note, the permeability threshold value for ECCS-based differentiation between classes 1/2 and 3/4 has so far not been intensively investigated.

For the accurate determination of low metabolic clearance values, the use of systems allowing for longer incubation times than primary hepatocytes in suspension (limited to 4–6 hours) is beneficial. HepatoPac is an example of a long-term human hepatocyte coculture system that maintains viability and functional expression of drug metabolizing enzymes for up to 7 days and is now well established (Khetani and Bhatia, 2008; Lin and Khetani, 2016), whereas other assay approaches, such as the Hurel microliver platform and relay method, are also available (Hultman et al., 2016; Murgasova, 2019). HepatoPac has been shown to provide improved accuracy and precision of hepatic intrinsic metabolic clearance predictions compared with hepatocytes in monoculture (Kratochwil et al., 2017; Chan et al., 2019; Docci et al., 2019).

In this study, ECCS classification and IVIVE for human CLint,h prediction was conducted for 36 marketed drugs with low-to-high in vivo clearance, which are substrates of metabolic enzymes and active uptake transporters in the liver. Metabolic intrinsic clearance CLint,h was estimated with HepatoPac and was compared with estimations made with suspended hepatocytes. Passive permeability measured in Lilly Laboratories Cell Porcine Kidney 1 (LLC-PK1) cells was compared with the ratio PSinf,active/PSinf in plated human hepatocytes for a training compound set, and a threshold permeability for ECCS-based compound classification was determined. Finally, a workflow for selection of the most appropriate in vitro tools for human CLh prediction was defined.

Materials and Methods

Chemicals and Biologic Materials. Bupropion, cimetidine, dextromethorphan, diclofenac, digoxin, fexofenadine, fluvastatin, furosemide, gemfibrozil, ketoconazole, irinotecan, MK-571, mycophenolic acid, pravastatin, propranolol, quinidine, tolbutamide, and verapamil were purchased from Sigma-Aldrich (St. Louis, MO). Oseltamivir, repaglinide, SN-38, memantine, and zosuquidar were obtained from Toronto Research Chemicals (Toronto, Canada). Atorvastatin, benzydamine, clozapine, famotidine, rosuvastatin, simvastatin, and valsartan were purchased from ChemPacific (Baltimore, MD), Honeywell Research Chemicals (Charlotte, NC), Memory Pharmaceuticals (Montvale, NJ), Prestwick Chemical (Illkirch, France), Cayman, LKT Laboratories (St. Paul, MN), and Lucerna Chem AG (Luzern, Switzerland), respectively. Cyclosporine A, efavirenz, and talinolol were provided by Syntex (Palo Alto, CA). Clopidogrel, ethynylestradiol, omeprazole, oxazepam [as internal standard for liquid chromatography–tandem mass spectrometry (LC-MS/MS) analysis], rosiglitazone, and midazolam were synthesized at F. Hoffmann-La Roche Ltd. (Basel, Switzerland). Acetonitrile and PBS were obtained from Biosolve Chimie (Dieuze, France) and

Thermo Fisher Scientific (Waltham, MA), respectively. DMSO (Sigma-Aldrich) was used to prepare stock solutions of the test drugs, resulting in 0.1% (v/v) DMSO concentrations in the final incubation samples.

Human cryopreserved hepatocytes for hepatic uptake and metabolism assays were obtained from BioIVT (Westbury, NY). Viability of hepatocytes after reconstitution was at least 80% throughout the study. Ready-to-use Human HepatoPac cultures (long-term hepatocyte cocultures; a pool of 10 donors) and stromal mouse fibroblasts (lots/donors: 8305/YFA and 9177/ACR; pooled) with the plates for incubations, application medium, and maintenance medium were acquired from BioIVT.

Passive Permeability in LLC-PK1 Cells. LLC-PK1 cells overexpressing human P-glycoprotein (encoded by the multidrug resistance 1 gene) were obtained from Dr. A. Schinkel, The Netherlands Cancer Institute (Amsterdam, The Netherlands) under license agreement and used for monolayer permeability measurements as previously described (Poirier et al., 2014). Cells were cultured in Medium-199 supplemented with 10% (v/v) fetal calf serum (FCS), penicillin-streptomycin (10,000 IU/μg per milliliter), and colchicine (150 ng/ml).

Briefly, compounds dosed at 1 μM in phenol red-free Medium-199 supplemented with 10% (v/v) FCS and penicillin-streptomycin (10,000 IU/μg per milliliter) were evaluated for permeability in the apical-to-basolateral and basolateral-to-apical directions using a liquid handling robot (Tecan, Männedorf, Switzerland). Samples were collected from triplicate wells of donor and receiver compartments after a 3.5-hour incubation in the presence or absence of P-glycoprotein (P-gp) inhibitor (zosuquidar, 1 μM). Drug concentrations were measured by high-performance LC-MS/MS. The extracellular marker lucifer yellow (10 μM) was also added to ensure monolayer integrity; values exceeding 25 nm/s were eliminated from analysis. The incubation was conducted in triplicates.

For the permeability data assessment, the following equation was used:

$$P_{app}(nm/sec) = \frac{1}{A \times C0} \times \frac{dQ}{dt} \quad (1)$$

where apparent permeability (P_{app}), A, C0, and dQ/dt represent the mean, bidirectional apparent permeability in the presence of P-gp inhibitor; the filter surface area; the initial concentration of test substances; and the amount per time period (3.5 hours), respectively. The recovery was calculated according to the following equation:

$$Recovery\ (\%) = \left(\frac{C_r V_r + C_d V_d}{C_{d0} V_d} \right) \times 100 \quad (2)$$

where C_r is the concentration in the receiver compartment at the end of experiment, V_r is the volume of the receiver compartment, C_d is the concentration in the donor compartment at the end of experiment, C_{d0} is the initial concentration in the donor compartment, and V_d is the volume of the donor compartment. The acceptable range for mass balance recovery was 70%–120%.

Hepatic Uptake in Human Plated Hepatocytes. The cryopreserved primary cells (male and female; mixed) were reconstituted in a tube containing prewarmed *InVitro*GRO cryopreserved platable medium at 37°C (BioreclamationIVT). To each well of a collagen I–coated 24-well tissue culture plate (BD BIOCOAT; BD Biosciences, San Jose, CA), 0.5 ml of the cell suspension was added corresponding to approximately a cell density of 0.3×10^6 cells per well. The plates were then incubated at 37°C and 5% CO_2, with saturating humidity for 3 and 4 hours to allow for cell adherence, the medium was removed, and the cells were washed once with 1 ml of prewarmed Hanks' balanced salt solution (HBSS; Thermo Fisher Scientific), supplemented with HEPES (20 mM), pH 7.4. The experiment was initiated by aspirating the wash buffer and then adding 0.3 ml of a prewarmed serum-free HBSS including the test compound in the absence and presence of the inhibitor cocktail on active transporters: MK-571 at 100 μM, cyclosporine A at 20 μM, and quinidine at 100 μM [inhibiting organic anion transporting polypeptides (OATPs), P-gp, breast cancer resistance protein (BCRP), MRPs, bile salt export pump, Na+-taurocholate cotransporting polypeptide, organic anion transporter (OAT) 2, and organic cation transporter (OCT) 1]. The inhibitor concentrations were optimized to achieve complete inhibition effects on hepatic transporters without any cell toxicity (in-house

TABLE 1

Data supporting ECCS classification of 36 marketed drugs and collected data on main elimination pathways

Table 1 summarizes physicochemical parameters used for the ECCS classification of 36 marketed drugs. The pathways (enzymes and transporters) involved in hepatic (and renal) elimination are provided. Pathway descriptions are provided in parentheses if the clinical relevance of the elimination pathways is not confirmed. Passive permeability (P_{app}) in the apical to basal direction in LLC-PK1 cells was measured in the present study or was taken from the literature (Caco-2 permeability) in the instances for which the reference is provided. Documentation for physiologically based pharmacokinetic models for the marketed drugs are provided with the SimCYP software platform and have been verified to show good performance for prediction of PK profiles and drug-drug interaction potential. Therefore, the model input parameters and drug disposition pathways were used for the current assessment.

No.	Compound	Molecular weight (g/mol)	Ionization classification at pH 7.4	P_{app} (A to B)		Main elimination pathways			ECCS
				(nm/s)	Reference	Enzyme	Transporter	Reference	
1	Midazolam	325.78	Base	135		CYP3A4	—	FDA, 2020	2
2	Quinidine	324.42	Base	280		CYP3A4	—	FDA, 2020	2
3	Dextromethorphan	271.40	Base	291		CYP2D6	—	FDA, 2020	2
4	Diclofenac	296.15	Acid	132.8	Lee et al., 2017	CYP2C9	—	FDA, 2020	1a
5	Tolbutamide	270.35	Acid	173		CYP2C9	—	FDA, 2020	1a
6	Bupropion	239.74	Base	388		CYP2B6	—	FDA, 2020	2
7	Propranolol	259.34	Base	287		CYP2D6/multiple	—	McGinnity et al., 2004	2
8	Verapamil	454.60	Base	197		CYP3A4	—	McGinnity et al., 2004	2
9	Clozapine	326.82	Base	199		CYP1A2/multiple	—	McGinnity et al., 2004	2
10	Efavirenz	315.68	Acid	158		CYP2B6/2A6 > 3A4 and 1A2	—	Simcyp	2
11	Rosiglitazone	357.43	Acid	152		CYP2C8/3A4	—	Simcyp	1a
12	Omeprazole	345.42	Neutral	253		CYP2C19/3A4	—	Simcyp	2
13	Ethinylestradiol	296.40	Neutral	233		CYP1A2/2C9/3A4, UGT1A1 and SULTs	—	Simcyp	2
14	Mycophenolic acid	320.34	Acid	50		UGT1A9/2B7	Minor/(MRP2)	Picard et al., 2005; Patel et al., 2017	1a
15	Clopidogrel	321.82	Base	257		CES1/CYP2C19	—	Polasek et al., 2011	2
16	Oseltamivir	312.40	Base	45		CES1	—	FDA review	3a
17	Irinotecan	586.68	Base	21		CES1/2/CYP3A	P-gp/MRP2	Mathijssen et al., 2001; Toshimoto et al., 2017	4
18	SN-38	392.40	Base	37		UGT1A1	P-gp/MRP2/BCRP	Mathijssen et al., 2001; Toshimoto et al., 2017	4
19	Benzydamine	309.41	Base	302		FMO(1/)3 (and UGT)	—	Baldock et al., 1990; Bohnert et al., 2016	2
20	Cyclosporine A	1202.60	Neutral	68		CYP3A4	(P-gp)	Simcyp; (Thiel et al., 2015)	2
21	Ketoconazole	531.43	Base	171		CYP3A4 (+UGT/FMO/deacetylation)	—	Kim et al., 2017	2
22	Atorvastatin	558.64	Acid	11		CYP3A4	OATP1B1	Maeda et al., 2011	3b
23	Fluvastatin	411.47	Acid	26	Li et al., 2011	CYP2C9	(OATP1B1/)BCRP	Fujino et al., 2004; Keskitalo et al., 2009; Kunze et al., 2014	3b
24	Simvastatin	418.57	Neutral	52		CYP3A4	(OATP1B1/1B3)	Simcyp; (Kunze et al., 2014)	2
25	Pravastatin	424.53	Acid	3.22		Minor	OATP1B1/MRP2	Thiel et al., 2015	3b
26	Rosuvastatin	481.54	Acid	0 (BLOQ)		Minor	OATP1B1/NTCP/BCRP	Simcyp	3b
27	Famotidine	337.45	Base	12		Minor (S-oxide formation)	OCT2 (renal)	Echizen and Ishizaki, 1991; FDA, 2020	4
28	Gemfibrozil	250.33	Acid	82		UGT2B7	—	Simcyp	1a
29	Fexofenadine	501.68	Zwitterions	0 (BLOQ)		—	OATP1B3 and unknown mechanism	Shimizu et al., 2005	3b
30	Memantine	179.30	Base	320		—	OCT2 (renal)	FDA, 2020	2
31	Repaglinide	452.59	Zwitterions	41		CYP3A4/2C8	OATP1B1	Drug label	3b
32	Furosemide	330.75	Acid	36		Biliary excretion	OAT3 (renal)	FDA, 2020	3a
33	Valsartan	435.52	Acid	0 (BLOQ)		P450 (minor)	OATP1B1/1B3/MRP2	Waldmeier et al., 1997; FDA, 2020	3b
34	Cimetidine	252.34	Base	35		P450 (minor)	OAT3/OCT2 (renal)	Somogyi and Gugler, 1983; McGinnity et al., 2004; FDA, 2020	4
35	Digoxin	780.94	Neutral	54	Zhang and Morris, 2003	Minor	P-gp	(Caldwell and Cline, 1976); Simcyp	2
				35–45					4
36	Talinolol	363.50	Base	29	Anderle et al., 1998	(CYP3A4)	P-gp (and MRP2)	Giessmann et al., 2004; FDA, 2020	4

BLOQ, below limit of quantification; NTCP, Na$^+$-taurocholate cotransporting polypeptide.

information). After the designated incubation time optimized to derive the linear uptake profile, the assay was stopped by washing the cells three times with ice-cold HBSS buffer containing 0.2% (v/v) bovine serum albumin. Subsequently, 0.3 ml of acetonitrile/water (75/25, v/v) containing internal standard was added to deprotonate the cells. The aliquot was transferred into LC-MS/MS to measure concentrations of the test drug. Using an additional cell plate by lysing the cells in 1% (v/v) Triton X-100, an average protein content (milligrams per milliliterl) was determined by the Pierce BCA assay kit with bovine serum albumin used as standard (Thermo Fisher Scientific). The uptake assay was conducted in triplicates.

Drug permeability clearance across the plasma membrane (PSinf: milliliters per minute per milligram protein) was determined from the test compound amount inside the cells (normalized to the cell protein amount and incubation time) divided by the measured concentration in the incubation

TABLE 2

Measured and scaled hepatic intrinsic clearance from the in vitro assays, in comparison with the respective in vivo data among 36 marketed drugs

Not detected: calculated values are below the internal resolution limit criteria (<0.1 µl/min per milligram). For IVIVE with the in vitro data, the following scaling factors were applied irrespective of differences of the two in vitro assay systems (hepatocyte suspension and HepatoPac): hepatocellularity, 120 (10⁶ cells = mg protein/g liver); liver weight, 22 (g liver/kgbw); and body weight, 70 (kgbw). These were generally derived from a system parameter database (Johnson et al., 2005). The in vivo intrinsic hepatic clearance was calculated with the well-stirred model, the in vivo CLh,p, and hepatic blood flow rate (23.2 ml/min per milligram; Johnson et al., 2005). For the marketed drugs, perfusion-limited conditions were applied even though permeability limitations in hepatic elimination may have been reported for some. Key PK parameters used to estimate the in vitro CLint,h.u (upscaled) and in vivo CLint,h.u (reference) were also provided in this table. Derivations of the in vivo CLtot,p are listed in Supplemental Table 1 with the respective literature source information. Documentation for physiologically based pharmacokinetic models for the marketed drugs are provided with the SimCYP software platform and have been verified to show good performance for prediction of PK profiles and drug-drug interaction potential. Therefore, the model input parameters and drug disposition pathways were used for the current assessment.

		$f_{u,p}$		R_b		$f_{u(inc)}^a$	In vitro				In vivo				
							$CL_{int,h}$ (hep sus)	$CL_{int,h.u}$	$CL_{int,h}$ (HepatoPac)	$CL_{int,h.u}$	$CL_{int,h.u}$	$CL_{h,p}$	$CL_{r,p}$	$CL_{others,p}$	$CL_{tot,p}$
No.	Compound	-	Ref.	-	Ref.	-	(µl/min per milligram)	(ml/min per milligram)	(µl/min per milligram)	(ml/min per kilogram)	(ml/min per kilogram)		(ml/min per kilogram)		
ECCS class 1a and 2^b															
1	Midazolam	0.0320	Simcyp	0.60	Simcyp	0.25	32.50	345.35	43.60	463.29	631.27	8.27	0.02	0.00	8.29
2	Quinidine	0.2020	Simcyp	0.82	Simcyp	0.72	2.59	9.54	12.50	46.04	52.34	6.80	1.67	0.00	8.47
3	Dextromethorphan	0.5000	Simcyp	1.32	Simcyp	0.91	9.60	27.88	13.70	39.78	57.00	14.76	0.00	0.00	14.76
4	**Diclofenac**	0.0038	Ye et al., 2016	0.55	Ye et al., 2016	0.04	3.10	222.73	4.30	308.95	561.90	1.83	2.74	0.00	4.57
5	**Tolbutamide**	0.0440	Simcyp	0.60	Simcyp	0.32	1.17	9.80	1.30	10.89	4.85	0.21	0.00	0.00	0.21
6	Bupropion	0.1600	Simcyp	0.82	Simcyp	0.66	0.70	2.82	27.10	109.10	119.20	9.52	0.00	0.00	9.52
7	Propranolol	0.0990	Poulin and Theil, 2002	0.89	Shibata et al., 2002	0.52	3.00	15.13	11.50	57.99	129.88	7.92	0.04	0.00	7.96
8	Verapamil	0.1000	Lombardo et al., 2004	0.77	Shibata et al., 2002	0.53	23.40	117.37	23.40	117.37	12,484.95	17.61	0.36	0.00	17.97
9	Clozapine	0.0550	Simcyp	0.85	Simcyp	0.37	5.00	35.88	12.90	92.57	43.40	2.13	0.0065	0.00	2.13
10	Efavirenz	0.0290	Simcyp	0.74	Simcyp	0.23	2.60	29.85	2.40	27.55	21.92	0.61	0.00	0.00	0.61
11	**Rosiglitazone**	0.0030	Simcyp	0.96	Simcyp	0.03	2.77	250.34	3.00	271.13	245.70	0.71	0.0007	0.00	0.71
12	Omeprazole	0.0430	Simcyp	0.59	Simcyp	0.31	6.30	53.65	25.60	218.00	90.69	3.04	0.01	0.00	3.04
13	Ethinylestradiol	0.0150	Simcyp	1.00	Simcyp	0.13	37.92	757.49	17.90	357.57	403.36	4.80	1.0011	0.00	5.80
14	**Mycophenolic acid**	0.0300	Bullingham et al., 1998	0.70	Malmborg and Ploeger, 2013	0.24	5.38	60.13	18.00	201.17	209.22	4.53	0.0158	0.00	4.54
ECCS class 3b^e															
15	Clopidogrel	0.0370	In silico pred.	1.00	—^c	0.28	200.00	1902.23	59.60	566.86	1229.14	15.36	0.00	0.00	15.36
19	Benzydamine	0.1460	Reddy et al., 2018	0.76	Reddy et al., 2018	0.63	2.63	11.00	5.50	23.01	7.04	0.97	1.31	0.00	2.29
20	Cyclosporine A	0.0365	Simcyp	1.62	Simcyp	0.27	3.10	29.79	10.30	98.97	460.25	11.61	0.01	0.00	11.62
21	Ketoconazole	0.0290	Simcyp	0.62	Simcyp	0.23	23.50	269.77	28.40	326.02	108.50	2.58	0.04	0.00	2.62
24	Simvastatin	0.0200	Simcyp	1.00	Simcyp	0.17	88.84	1383.77	49.70	774.13	422.83	6.20	0.92	0.00	7.12
28	**Gemfibrozil**	0.0080	Simcyp	0.75	Simcyp	0.07	2.34	82.78	8.10	286.55	159.50	1.19	0.01	0.09^d	1.28
30	Memantine	0.5500	Product monograph_Lundbeck	1.00	Product monograph_Lundbeck	0.92	Not detected	0.00	0.50	1.43	0.71	0.39	1.82	0.00	2.20
35	Digoxin	0.7100	Simcyp	1.07	Simcyp	0.96	Not detected	0.00	0.70	1.92	1.97	1.32	2.48	0.00	3.80
22	Atorvastatin	0.0570	Waldmeier et al., 1997	0.68	PMDA database	0.38	1.29	9.04	9.90	69.38	179.64	6.21	0.00	0.55	6.75^f
23	Fluvastatin	0.0100	Tse et al., 1993	0.71	Tse et al., 1993	0.09	Not detected	0.00	19.20	552.50	401.46	3.23	0.33	2.54	6.10^f
25	Pravastatin	0.4850	Simcyp	0.56	Simcyp	0.90	1.00	2.92	0.40	1.17	22.15	5.86	4.60	0.00	10.47
26	Rosuvastatin	0.1070	Simcyp	0.63	Simcyp	0.55	1.24	6.01	1.20	5.81	186.86	8.40	3.24	0.00	11.64
29	Fexofenadine	0.3000	Product monograph_Sanofi (a median of the range; in vivo fu,p)	1.00	—^c	0.81	Not detected	0.00	0.10	0.33	8.04	2.19	0.91	0.00	3.10
31	Repaglinide	0.0230	Simcyp	0.62	Simcyp	0.19	3.38	46.83	8.80	121.92	1057.47	9.04	0.01	0.00	9.05
33	Valsartan	0.0560	Simcyp	0.56	Simcyp	0.37	0.30	2.13	0.40	2.84	6.87	0.37	0.15	0.00	0.52
ECCS class 3a and 4^g															
16	**Oseltamivir** (prodrug)	0.8130	In silico pred.	1.00	In silico pred.	0.98	25.72	69.46	19.50	52.66	204.91	20.36	6.17	0.00	26.53
17	Irinotecan	0.2980	Toshimoto et al., 2017	0.81	Toshimoto et al., 2017	0.81	0.80	2.61	3.30	10.76	32.01	6.70^h	1.87	0.00	8.57
18	SN-38	0.0283	Toshimoto et al., 2017	1.31	Toshimoto et al., 2017	0.23	0.50	5.85	6.60	77.25	264.80^h	—	—	—	—

TABLE 2—Continued

No.	Compound	fu,p	Ref.	Rb	Ref.	fu(inc)[a]	In vitro CLint,h (hep sus)	In vitro CLint,h,u	In vitro CLint,h (HepatoPac)	In vitro CLint,h,u	In vivo CLint,h,u	In vivo CLh,p	In vivo CLr,p	In vivo CLothers,p	In vivo CLtot,p
		-		-		-	(μL/min per milligram)	(ml/min per milligram)	(μl/min per milligram)	(ml/min per kilogram)	(ml/min per kilogram)	(ml/min per kilogram)			
27	Famotidine	0.8105	(Echizen and Ishizaki, 1991) (a median of the range; in vivo fp)	1.00	—[c]	0.98	Not detected	0.00	Not detected	0.00	1.82	1.38	3.63	0.00	5.01
32	**Furosemide**	0.0240	Camenisch and Umehara, 2012	0.75	Camenisch and Umehara, 2012	0.20	Not detected	0.00	0.00	0.00	8.31	0.20	0.71	1.06[i]	1.97
34	Cimetidine	0.7785	(Somogyi and Gugler, 1983) (mean of the range)	0.98	Somogyi and Gugler, 1983	0.97	Not detected	0.00	0.50	1.36	6.09	3.92	6.81	0.00	10.74
36	Talinolol	0.3000	Thiel et al., 2015	1.00	—[c]	0.81	1.00	3.26	4.50	14.65	7.70	2.10	2.80	0.00	4.90

[a]Predicted with dilution method (Schuhmacher et al., 2000) using the respectively reported or measured unbound fractions in plasma. In hepatocyte suspension and HepatoPac assays, 10% FCS was added to the incubation media.
[b]ECCS class 1a (n = 5, in bold) and class 2 (n = 17, in bold) and class 2 (n = 17; primarily elimination = metabolism.
[c]Informed assumption since there is no literature information available.
[d]Contribution of UGT2B7 in kidney (Simcyp).
[e]ECCS class 3b (n = 7): primarily elimination = hepatic uptake (or renal excretion).
[f]Estimation using Simcyp to capture the plasma concentration profiles over time.
[g]ECCS class 3a (n = 2, in bold) and class 4 (n = 5): primarily elimination = renal excretion.
[h]Estimation with physiologically based PK modeling using top-down approach (Toshimoto et al., 2017).
[i]Contribution of biliary excretion.

medium. Contribution of an active uptake (PSinf,act) component (%) to the total permeability clearance (PSinf) was calculated with the following equation:

$$(1 - a \text{ ratio dividing the drug permeability clearance with and} \\ \text{without the inhibitor cocktail } (PSinf,pas/PSinf)) \times 100 \quad (3)$$

ECCS Classification of Marketed Drugs Based on an Experimentally Defined Permeability Threshold. Using Roche in-house synthesized discovery compounds from the same chemical series as a development compound previously reported to show active hepatic uptake in clinical studies (Kratochwil et al., 2018), P_{app} (nanometers per second) in the apical to basal direction in LLC-PK1 cells was plotted against the respective hepatic active uptake component (%). These compounds all included a carboxylic acid moiety, indicating potential of being substrates of OATP, and had MW >400. This correlation was used to set a permeability threshold for ECCS-based differentiation between classes 1/2 and 3/4. For verification, ECCS classification for 36 marketed drugs was conducted, followed by IVIVE for CLint,h prediction. Known enzyme and transporter interactions for these drugs are provided in Table 1.

Metabolism by Suspended Human Hepatocytes. Primary pooled cryo-preserved hepatocytes (male and female; mixed) were reconstituted in prewarmed William's E media containing 10% FCS, 0.05 mg/ml streptomycin and 50 U/ml penicillin, and 0.4 mM L-glutamine from Thermo Fisher Scientific and 0.01 mg/ml gentamicin, 0.048 mg/ml hydrocortisone, and 0.004 mg/ml insulin from Sigma-Aldrich, to a final suspension density of 1×10^6 cells/ml.

The incubation was performed fully automatically with Evo Liquid Handling System (Tecan) equipped with a CO_2 incubator with an orbital shaker from LiCONiC instruments (Montabaur, Germany). After the addition of test compounds at 1 μM, 0.1% v/v DMSO (marketed: n = 36) to the wells (1 × 10^5 cells/well, 100 μl incubation volume), the 96-well hepatocyte suspension culture plates were incubated at 900 rpm in a 5% CO_2 at 37°C. Samples were quenched by addition of acetonitrile (including an internal standard) to the incubation well at the designated time points up to 2 hours. The incubation was conducted in n = 1 or 2. For intrinsic clearance, n = 1 denotes a single intrinsic clearance value determined using seven different independent incubation wells with different incubation times.

The natural logarithm of the percentage initial drug concentration in the incubation samples was plotted against time, and a linear regression analysis was applied using GraphPad Prism version 7.04 for Windows (GraphPad Software, La Jolla, CA). The in vitro CLint was calculated from the slope of the linear regression:

$$In \text{ } Vitro \text{ } CL_{int}(\mu L/min/10^6 \text{ } hepatocytes) = \frac{-slope * V_{incubation} * 10^6}{n_{hepatocytes \text{ } per \text{ } incubation}} \quad (4)$$

A conversion factor of 1 mg protein per million hepatocytes as determined previously (Kratochwil et al., 2017) was used to convert intrinsic clearance per million cells into intrinsic clearance per milligram hepatocyte protein.

Metabolism by Human HepatoPac. Incubations for the same set of the test compounds (1 μM, 0.1% v/v DMSO) as conducted in suspension assays were performed in 96-well plates containing either a coculture of adherent hepatocytes (mixed, n = 5 for male and n = 5 for female) with mouse fibroblast control cells or control cells alone (5% CO_2 atmosphere and 37°C). The incubation media in human HepatoPac was identical with that in suspended hepatocytes. At defined time points (2, 18, 26, 48, 72, and 96 hours), whole wells were quenched with ice-cold acetonitrile containing an internal standard. Samples were then centrifuged appropriately, and the supernatant was analyzed by LC-MS/MS. The incubation was conducted in n = 1 or 2. For intrinsic clearance, n = 1 denotes a single intrinsic clearance value determined using eight different independent incubation wells with different incubation times.

Measured concentrations in the medium were plotted against incubation time (minutes) and a linear fit made to the data with emphasis upon the initial rate of compound disappearance. This calculation was performed for samples prepared from HepatoPac and fibroblast control cells (stromal cells). The slope of the fit was then used to calculate the apparent intrinsic clearance:
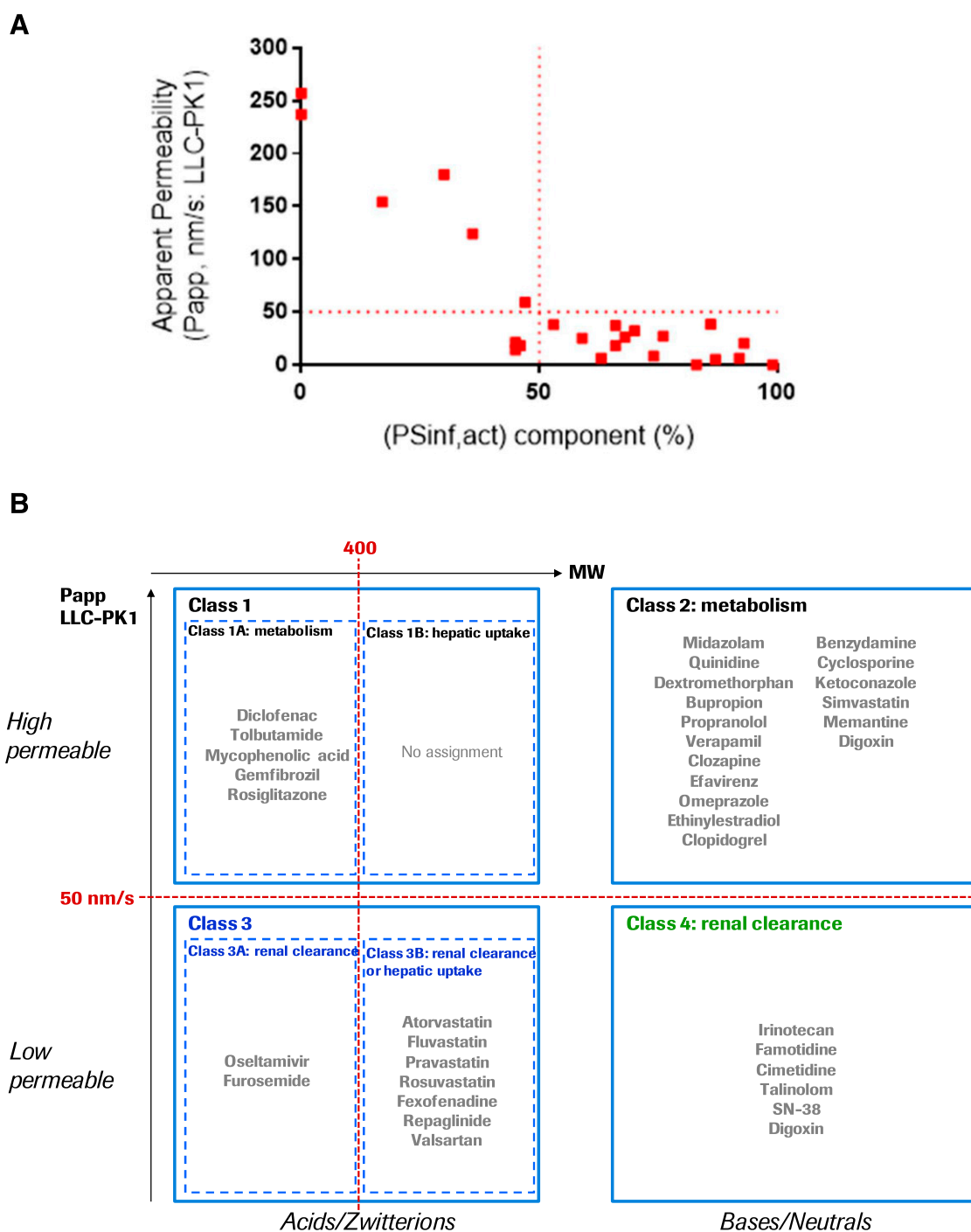
A

B

Fig. 1. Comparison of apparent permeability in LLC-PK1 cells to active uptake in human hepatocytes. (A) P_{app} values (nanometers per second) in the apical to basal direction in LLC-PK1 cells are plotted against active uptake component in plated hepatocytes for a set of discovery compounds (MW > 400) with a carboxylic acid moiety. Each data point is as expressed an average of triplicate measurements for one compound. (B) ECCS classification of the 36 marketed drugs used for CLint,h,u prediction. ECCS class 1b compounds in parentheses represent the assignment according to Varma et al. (2015). Digoxin can be assigned to ECCS class 2 or class 4 depending on reported P_{app} values (Table 1).

$$CLint, met, app \ (\mu L/min/mg \ protein) = [slope \ (min^{-1}) \times 1000] \ / \ protein \ concentration \ (mg \ protein/mL) \quad (5)$$

The apparent intrinsic clearance in hepatocytes was corrected for fibroblast metabolism. Each well in HepatoPac plates has 75% surface area as fibroblasts and 25% surface area as hepatocytes (Khetani and Bhatia, 2008; Chan et al., 2019). The in vitro intrinsic clearance determined from the fibroblast lysate according to eq. 5 were multiplied by 0.75 and then subtracted from the respective value determined in HepatoPac plates, to exclude metabolic clearance by fibroblasts. Hence,

the hepatocyte-specific intrinsic clearance (CLint,met) was calculated using eq. 6:

$$Hepatocytes \ CLint, met \ (\mu L/min/mg \ protein)$$
$$= HepatoPac \ CLint, met, app \ (\mu L/min/mg \ protein) - (0.75$$
$$\times \ Fibroblasts \ (stromal \ cells) \ CLint \ (\mu L/min/mg \ protein)) \quad (6)$$

LC-MS/MS Analysis. Calibration samples for test compounds were prepared by spiking stock solution of the test substance into the blank culture medium used
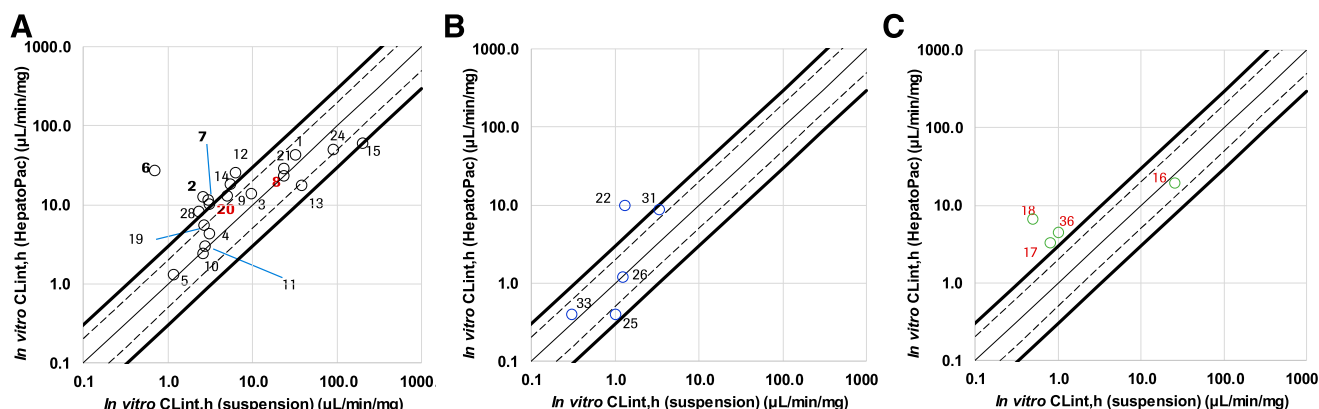
Fig. 2. Apparent in vitro intrinsic clearance for marketed drugs measured in suspended human hepatocytes and HepatoPac. For 36 marketed drugs at 1 μM, apparent in vitro intrinsic clearance CLint,h [without correction by unbound fraction in incubates fu(inc)] generated with suspended hepatocytes are compared with these generated in the HepatoPac model. The CLint,h values are calculated based on linear depletion rate of the parent drug from the media during the incubation time: 2 hours for hepatocyte suspension and 96 hours for HepatoPac (n = 1 or 2). For intrinsic clearance, n = 1 denotes a single intrinsic clearance value determined using seven (suspended hepatocytes) or eight (HepatoPac) different independent incubation wells with different incubation times. A hepatocyte cell density of 1.0 mg protein/10^6 cells is assumed irrespective of the two different assay systems (hepatocyte suspension and HepatoPac). CLint,h values of 20 compounds assigned as ECCS class 1a and 2 (i.e., predicted to be eliminated mainly by metabolism), five compounds as ECCS class 3b (i.e., likely eliminated mainly by hepatic active uptake and/or renal excretion), and remaining four compounds as ECCS class 3a and 4 (i.e., likely eliminated mainly by renal excretion) are plotted in (A–C), respectively. Compound names with numbering for each plot are summarized in Table 1. CLint,h values for 23. fluvastatin, 27. famotidine, 29. fexofenadine, 30. memantine, 32. furosemide, 34. cimetidine, and 35. digoxin are not shown due to a lack of measurement of depletion of the drug concentration from the media in suspended hepatocytes (Table 2). Solid, broken, and bold lines represent 1:1, 1:2, and 1:3 correspondence, respectively.

for the experiment (1%, v/v, DMSO), followed by quenching with 2-fold volumes of acetonitrile containing 0.1 μg/ml oxazepam as internal standard. All samples were 10-fold diluted in a mixture of acetonitrile and water (66:33, v/v). The high-performance liquid chromatography system consisted of 20AD Shimadzu pumps (Kyoyo, Japan) and an HTS CTC PAL autosampler (CTC Analytics AG; Zwingen, Switzerland). Sample solutions (1 μl) were injected into the analytical column heated to 60°C (Supelco Ascentis Express C18; 2 cm × 2.1 mm, particle size: 2.7 μm; Sigma-Aldrich). To elute the compounds, the following mobile phases were used: phase A, formic acid 0.5% in water:methanol = 95:5 (v/v); phase B, acetonitrile. A high pressure linear gradient from 0% to 95% B in 40 seconds was applied at a flow rate of 600 μl/min. Mass spectrometric detection with multiple reaction monitoring was operated in the positive ion mode with an API6500 mass spectrometer equipped with a TurboIonSpray source (IonSpray Voltage 5500 V; Sciex, Framingham, MA). Analyst 1.6.3 software (Sciex) was used for data processing using linear regression with $1/x^2$ weighting on peak area ratio. The precision and accuracy of linear regression of the standard curve samples was between 80% and 120%.

Prediction of Human Hepatic Intrinsic Clearance from the In Vitro Assays. Using the measured clearance values (CLint,met from hepatocyte suspension and HepatoPac), the intrinsic hepatic unbound clearance (CLint,h,u) was estimated according to eq. 7:

$$CLint, h, u = \frac{CLint, met}{fu(inc)} = CLint, met, u \qquad (7)$$

where fu(inc) is the unbound fraction in incubates. The fu(inc) values were predicted with the dilution method (Schuhmacher et al., 2000) based on the reported unbound fractions in plasma (fu,p), without conducting experimental measurements (Table 2). Correspondence of calculated and measured fu(inc) values was confirmed with a limited test compound set (midazolam, quinidine, diclofenac, tolbutamide, and dextromethorphan) for which measured fu(inc) values were previously available: 0.19, 1, 0.02, 0.35, and 1, respectively (Kratochwil et al., 2017). This provided validity of the use of the dilution method for fu(inc) prediction. For measured intrinsic uptake clearance (PSinf), fu(inc) was assumed as 1, since the assays were conducted in the absence of serum protein.

It was assumed that intrinsic process clearance values in the current in vitro assays were measured under linear conditions: substrate concentration (S) << Km.

For CLint,h,u prediction, the following physiologic scaling factors were applied: hepatocellularity, 120 (10^6 cells = mg protein/g liver); liver weight, 22 (g liver/kgbw); and body weight, 70 (kgbw). The previous study results from the protein determination using human hepatocyte suspensions indicated that the 10^6

cells was equivalent to 1 mg protein content (Kratochwil et al., 2017). The identical relationship between milligrams protein and cell numbers is assumed with HeatoPac, which the identical protein content per hepatocyte is applied for scaling the hepatocyte CLint,met after subtraction of the background turnover measured by the incubation with fibrobrasts as indicated in eq. 6. Otherwise, the scaling factors were generally taken from the system parameter database (Johnson et al., 2005).

Estimation of Human In Vivo Hepatic (Intrinsic) Clearance as Reference. Pharmacokinetic parameters for reference compounds were collected from publications, clinical pharmacology review documents and drug prescribing labels. Hepatic plasma (organ) clearance CLh,p was calculated from total plasma clearance CLtot,p by subtraction of renal CLr,p and other pathway clearances CLothers,p:

$$CLh, p = CLtot, p - CLr, p - CLothers, p. \qquad (8)$$

The fu,p and the blood-to-plasma concentration ratio (Rb) were used for the calculation of $fu,b = fu,p/Rb$, assuming Rb = 1 if no data were available (Table 2).

Hepatic organ blood clearance (CLh,b) was obtained as $CLh,b = CLh,p/Rb$. Finally, the in vivo intrinsic hepatic clearance was calculated with the well stirred model as follows:

$$In\ vitro\ CLint, h, u = \frac{CLh, b}{fu, b \cdot \left(1 - \frac{CLh, b}{Qh}\right)} \qquad (9)$$

where Qh is hepatic blood flow rate (23.2 ml/min per kilogram; Johnson et al., 2005). Key pharmacokinetic (PK) parameters used for evaluation of the current IVIVE performance for CLint,h,u prediction are summarized in Table 2. Derivations of the in vivo CLtot,p, CLr,p, and CLothers,p are summarized in Supplemental Table 1 with the literature source information.

Results

ECCS Classification. P_{app} values (nanometers per second) in the apical-to-basal direction in LLC-PK1 cells were plotted against the active uptake component in plated hepatocytes for the training data set compounds (MW > 400), each containing a carboxylic acid moiety (Fig. 1A; Supplemental Table 2). The same compounds were incubated with plated hepatocytes in the absence and presence of the inhibitor cocktail for active transporters: MK-571 at 100 μM, cyclosporine A at 20 μM, and quinidine at 100 μM.
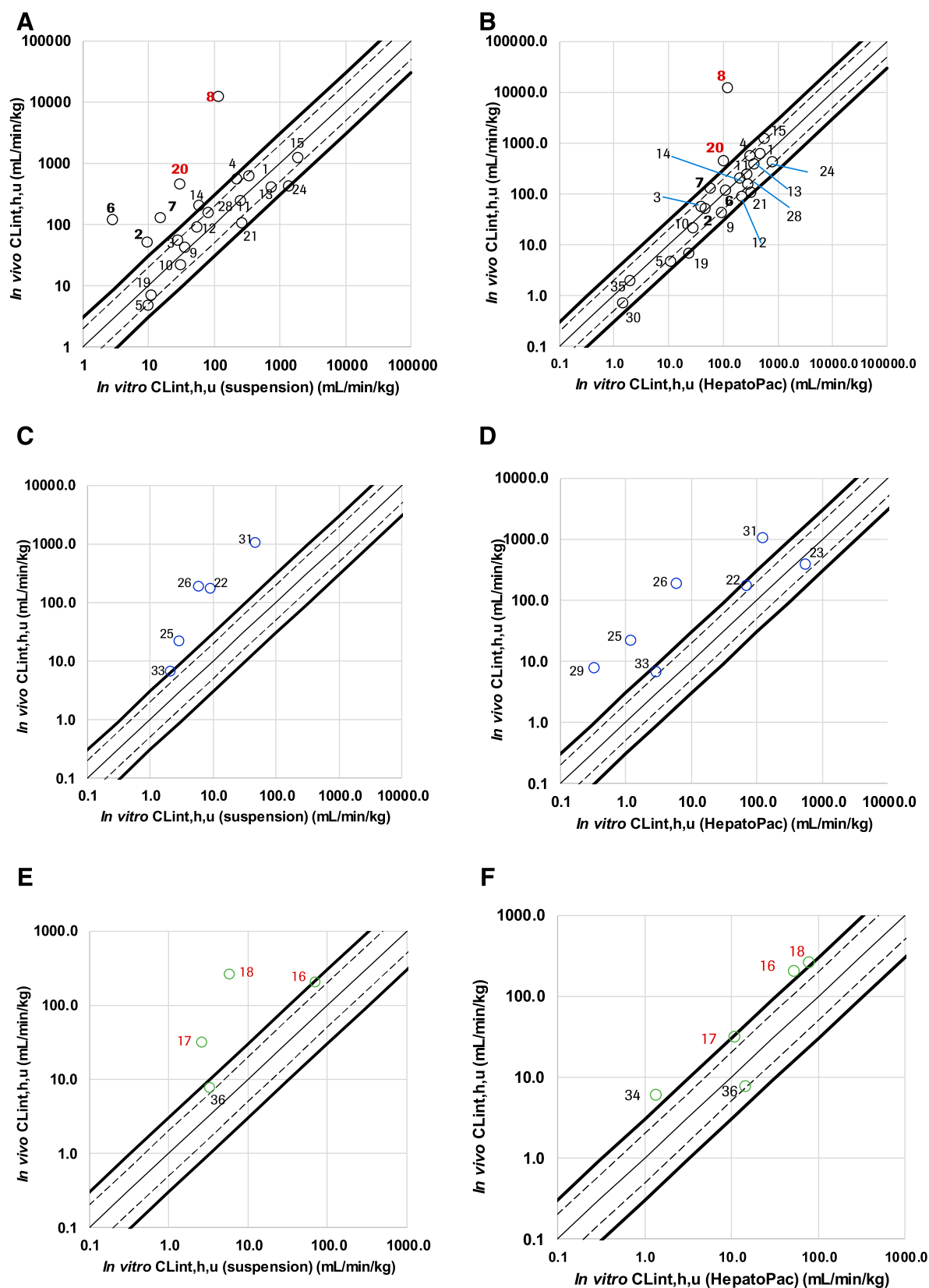
Fig. 3. Comparison of the reference and scaled-up hepatic intrinsic clearance values for marketed drugs. The in vivo CLint,h,u values (milliliters per minute per kilogram) for 36 marketed drugs are plotted against the in vitro CLint,h,u values (milliliters per minute per kilogram) from human suspended hepatocytes (A, C, and E) and HepatoPac (B, D, and F) assays. Twenty ECCS class 1a/2 compounds (i.e., predicted to be eliminated mainly by metabolism), five ECCS class 3b compounds (i.e., likely eliminated mainly by hepatic active uptake and/or renal excretion), and remaining four ECCS class 3a/4 compounds (i.e., likely eliminated mainly by renal excretion) are shown in panels (A–F), respectively. The in vitro and in vivo CLint,h,u values to illustrate the panels are listed in Table 2. Solid, broken, and bold lines represent 1:1, 1:2, and 1:3 correspondence, respectively.

Based on the internal compound set of active uptake substrates, a P_{app} value of 50 nm/s can be considered as a threshold above which active uptake was likely to be low, but below which net active uptake was likely to be important in the clearance of carboxylic acid–containing drugs (Fig. 1A). Thus, a threshold P_{app} of 50 nm/s is proposed here for ECCS subclassification to separate high (class 1 and 2) from low permeability compounds (class 3 and 4). Using this threshold, the 36 marketed drugs used for $CL_{int,h,u}$ prediction were classified as follows: five compounds in class 1a, 17 in class 2, two in class 3a, seven in class 3b, and five in class 4 (Fig. 1B; Table 1). No assignment was made to class 1b.

IVIVE for ECCS Class 1a/2 Compounds. Hepatic metabolism was estimated to be the predominant pathway for 22 out of the 36 marketed drugs (Fig. 1B; Table 1). The disposition pathway characterization was in agreement with the in vivo information on factors contributing to $CL_{h,p}$ (Table 2), except for memantine (No. 30) and digoxin (No. 35) for which renal clearance was actually the major pathway. Digoxin can be assigned to ECCS class 4 depending on historical P_{app} values (Table 1). In vitro $CL_{int,h}$ in HepatoPac was higher (by ≤3-fold) compared with that in suspended hepatocytes, especially when the intrinsic clearance was less than 10 μl/min per milligram in suspended hepatocytes (Fig. 2A; Supplemental Fig. 1; Table 2).

For quinidine (No. 2), bupropion (No. 6), propranolol (No. 7), and cyclosporine A (No. 20) with relatively low in vitro $CL_{int,h}$, a >3-fold underestimation of the upscaled $CL_{int,h,u}$ (milliliters per minute per kilogram) from the hepatocyte suspension assays relative to the reference in vivo $CL_{int,h,u}$ was observed (Fig. 3A; Table 2). HepatoPac assays improved the prediction performance, resulting in 2–3-fold errors (Fig. 3B; Supplemental Fig. 2; Table 2). IVIVE performance remained poor for verapamil (No. 8) irrespective of the assay.

IVIVE for ECCS Class 3b Compounds. Hepatic active uptake and renal excretion were estimated to be the main pathways for seven marketed drugs (class 3b; Fig. 1B; Supplemental Fig. 1; Table 1). Contribution of renal excretion to total elimination was indicated for fluvastatin (No. 23), pravastatin (No. 25), rosuvastatin (No. 26), fexofenadine (No. 29), and valsartan (No. 33, Table 2). Upscaled $CL_{int,h,u}$ (milliliters per minute per kilogram) was underestimated (by <10-fold) for several drugs (No. 25. pravastatin, No. 26. rosuvastatin, No. 29. fexofenadine) likely due to uptake clearance not contributing to hepatocyte metabolic clearance assessments (Fig. 3, C and D; Supplemental Fig. 2; Table 2). For these drugs, determination of PSinf using plated hepatocytes with short-term incubation (1–5 minutes) reveals an improved prediction of $CL_{int,h,u}$ (Supplemental Table 3).

$CL_{int,h,u}$ values for three compounds (No. 22. atorvastatin, No. 23. Fluvastatin, and No. 33. valsartan) were reasonably predicted with HepatoPac (within 2–3-fold errors) (Fig. 3D; Supplemental Fig. 2; Table 2).

IVIVE for ECCS Class 3a/4 Compounds. Renal excretion was estimated to be the main pathway for seven marketed drugs (Fig. 1B; Supplemental Fig. 1; Tables 1 and 2). Based on literature data, the relative contribution of $CL_{r,p}$ to total clearance was 23% for oseltamivir (No. 16), 33% for irinotecan (No. 17), 72% for famotidine (No. 27), 36% for furosemide (No. 32), 63% for cimetidine (No. 34), and 57% for talinolol (No. 36; Table 2). An occurrence of renal excretion of SN-38 (No. 18, an active drug of irinotecan) was qualitatively reported (Toshimoto et al., 2017) (Table 2). Relatively good prediction of $CL_{int,h,u}$ for ECCS class 3a and 4 compounds was shown with HepatoPac (Fig. 3, E and F and Supplemental Fig. 2).

Discussion

Usefulness of the ECCS (Varma et al., 2015) to estimate the rate-determining steps of a compound at the drug discovery stage is confirmed again in this study using a different set of marketed drugs for which drug disposition pathways are well known (Table 1). To identify whether metabolism or active transport is the rate-determining step in hepatic elimination, it is important to define an in vitro permeability filter for ECCS classification. A P_{app} threshold of 50 nm/s across LLC-PK1 monolayers is proposed in this study (Fig. 1A), corresponding to an active contribution to total hepatocyte uptake of ≥50% as measured in a plated hepatocyte assay. Independent of the current study, the same permeability threshold of 50 nm/s in low efflux Madin-Darby canine kidney cells and in Caco-2 cells was used for absorption and systemic clearance predictions based on ECCS classification (Fredlund et al., 2017; Varma et al., 2017).

The assignment to ECCS classification categories is straightforward; however, it may not always accurately predict the major rate-determining steps. For instance, digoxin (No. 35) is predominantly eliminated by the kidneys (Table 2). Actually, historical P_{app} values of digoxin measured in-house range from 35 to 45 nm/s below the threshold value, would result in ECCS class 4 assignment (Table 1). However, a reported P_{app} of digoxin was 54 nm/s, which is on the border of the threshold permeability (Zhang and Morris, 2003), resulting in an assignment to ECCS class 2 indicating predominant metabolism. These findings indicate the importance of accurate and precise P_{app} measurements by ensuring adequate experimental design (i.e., test within solubility range and under linear, sink conditions) and excluding the potential effects of nonspecific binding, transporter contribution, and poor mass balance as a consequence of cellular accumulation due to lysosomal trapping (Riede et al., 2019; Bednarczyk and Sanghvi, 2020). Furthermore, although we have determined a P_{app} threshold (50 nm/s) that is common with two other independent laboratories (as noted above), there remains the possibility of significant differences in P_{app} between other laboratories and in vitro systems. Left unchecked, the assumed rate-determining steps could be incorrectly assigned and would risk an inappropriate absorption, distribution, metabolism, and excretion strategy. To address this, we would recommend each group conduct its own assay calibration with reference compounds to either validate our proposed P_{app} threshold or to adjust accordingly.

This study confirmed that HepatoPac predicted hepatic intrinsic clearance with improved accuracy and precision compared with suspended hepatocytes, irrespective of hepatic clearance classification and ECCS class assignments (Fig. 3; Supplemental Fig. 2). Of note, an advantage of the use of HepatoPac was especially apparent for the low hepatic clearance compounds: quinidine (No. 2), bupropion (No. 6), and cyclosporine A (No. 20) in the ECCS classes 1 and 2 and irinotecan (No. 17), SN-38 (No. 18), cimetidine (No. 34), and talinolol (No. 36) in ECCS classes 3a and 4 (Fig. 3; Table 2). In addition, internal compounds showing an identical $CL_{int,h}$ in suspended hepatocytes of ~1 μl/min per milligram have sometimes showed up to 30-fold range in their HepatoPac $CL_{int,h}$ from 0.1 to 3 μl/min per milligram (in-house data), indicating improved sensitivity to low $CL_{int,h}$ determination in HepatoPac.

For ECCS class 3b drugs as atorvastatin (No. 22), fluvastatin (No. 23), and valsartan (No. 33), hepatic elimination might be governed by metabolism as well as uptake process, which is confirmed by the reasonable $CL_{int,h,u}$ prediction with 2–3-fold errors seen in HepatoPac (Fig. 3D; Table 2) and in hepatocytes for short incubation period, respectively (Watanabe et al., 2010; Umehara and Camenisch, 2012). Although $CL_{met,u}$ estimation for repaglinide (No. 31, due to CYP3A4 and CYP2C8) using HepatoPac is likely reliable relative to suspended hepatocytes, the in vitro $CL_{int,h}$ in HepatoPac shows an ~9-fold underestimation of the upscaled $CL_{int,h,u}$. It is likely that HepatoPac does not fully capture the hepatic uptake clearance seen in vivo (e.g., via OATP1B1, Fig. 3, C and D; Tables 1 and 2).
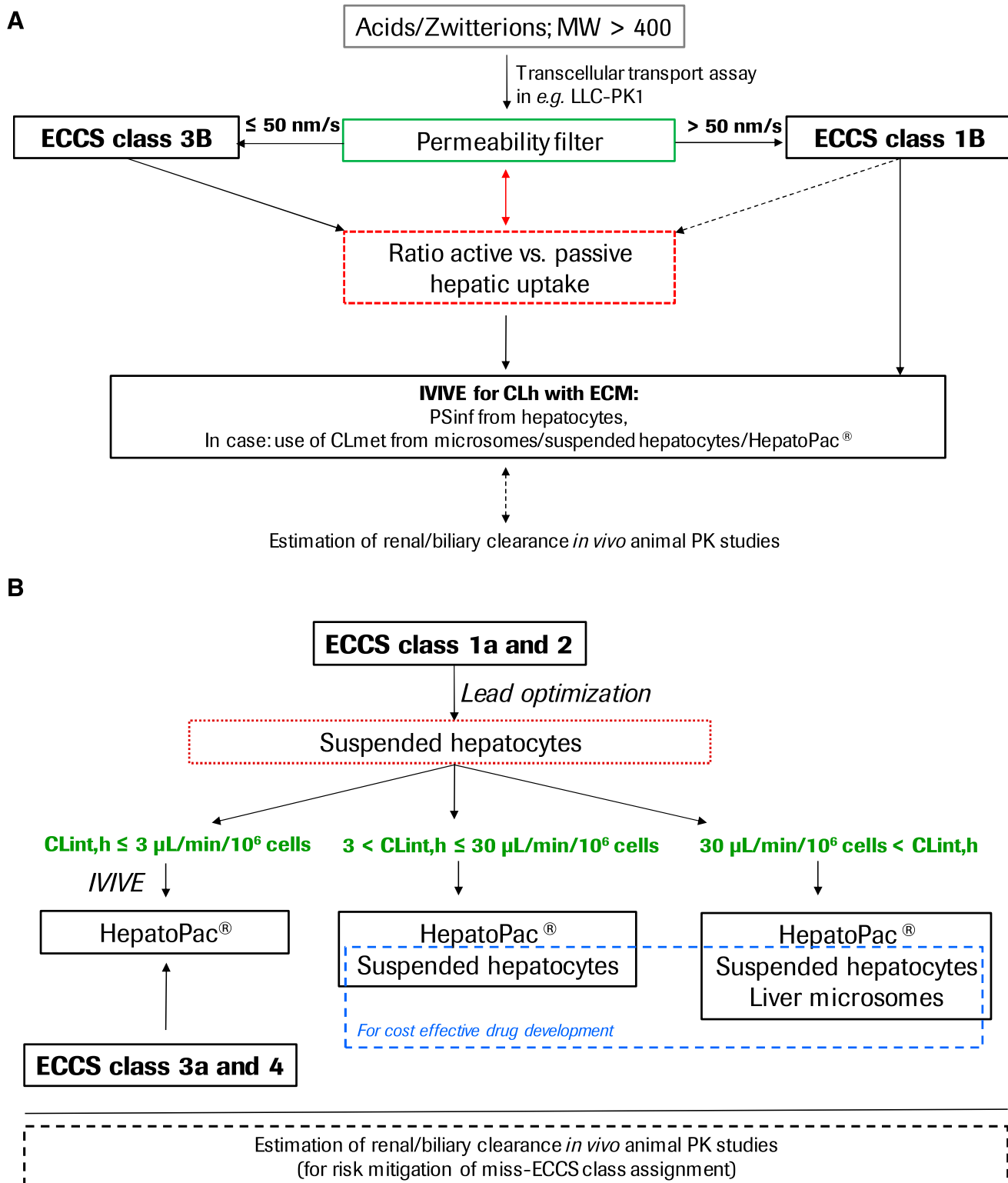
A

B

Fig. 4. Decision trees for the selection of the optimal in vitro assays for the in vitro to in vivo extrapolation of human hepatic clearance by active uptake and metabolism. The decision tree suggests an ECCS class-dependent selection of the optimal in vitro assay (liver microsomes, hepatocytes, and HepatoPac). The assessment of uptake and metabolic clearance processes is followed by IVIVE to predict the hepatic clearance. (A and B) represent decision trees for ECCS class1b/3b and ECCS class 1a/2/3a/4 compounds, respectively. The two schemes also indicate when the potential investigation of other disposition pathways such as biliary and renal excretion may be mandated. To compensate differences of human hepatocytes and liver microsomes for clearance optimization, hepatocellularity (120×10^6 cells/g liver) and liver microsomal contents (38 mg human liver microsome/g liver; Johnson et al., 2005) can be used.

None of the 36 reference drugs was assigned to class 1b (Fig. 1B; Table 1). Although atorvastatin, fluvastatin, and repaglinide were originally assigned to class 1b with the P_{app} threshold of 50 nm/s in low efflux Madin-Darby canine kidney cells (Varma et al., 2015), this study results reassigned these drugs in class 3b with the identical P_{app} threshold of 50 nm/s in LLC-PK1 cells. The inconsistent ECCS class assignment among substrates of active uptake transporters could be derived from the difference of the in vitro permeability assay format among test facilities. Irrespectively, previously reported ECCS class 1b compounds (bosentan, cerivastatin, glyburide, pitavastatin, and telmisartan) are subject to active uptake via OATPs and metabolism via CYP3A, CYP2Cs, and UDP-glucuronosyltransferases (UGTs) (Varma et al., 2015). The hepatic intrinsic clearance of ECCS class 3b/1b drugs (active transporter substrates with low metabolic turnover) can be successfully calculated using PSinf measured in hepatocytes (short-term incubation) and CLmet,u in HepatoPac by following previously reported calculations with marketed drugs (Watanabe et al., 2010; Umehara and Camenisch, 2012).

For ECCS class 3a/4 compounds, the contribution of CLr to total systemic clearance is predicted to be ≥70% (Varma et al., 2015), which implies that hepatic metabolism should account for below 30%, potentially indicating low metabolic turnover. Therefore, better prediction performance of CLint,h,u with HepatoPac was expected, and this is supported for the ECCS class 3a/4 compounds in this study (Fig. 3, E and F). However this type of molecule remains challenging since CLr,p contributes significantly to overall clearance (Table 2), and, with a few exceptions, verified IVIVE methods have not been established for this process. For example, prediction of renal secretion clearance of OAT substrates is demonstrated by estimating relative activity factors for the probe substrates of OATs to directly relate the in vitro transport clearance using the transporter-transfected human embryonic kidney cells to in vivo secretory clearance (Mathialagan et al., 2017). A model for prediction of extent of passive tubular absorption in the kidney is recently reported as a function of Caco-2 permeability (Scotcher et al., 2016).

Accordingly, a workflow for selection of in vitro tools to achieve optimal IVIVE prediction for hepatic clearance and identify the most relevant tools for clearance optimization can be proposed as shown in Figure 4. The workflow is different for ECCS class 1b/3b compounds with hepatic active transport, compared with class 1a/2/3a/4 compounds with hepatic metabolism, irrespective of the degree of the contribution of renal (and biliary) excretion to total elimination. Ongoing assessments of permeability are also important to ensure that relevant optimization targets continue to be set as lead series chemistry changes. Once compounds are identified as ECCS class 3b, a ratio of active and passive uptake clearance from the short-term incubation assays with hepatocytes could be measured to perform spot checks whether the ECCS class properties are maintained during the lead optimization phase (Fig. 4A). After the compound nomination, the in vitro uptake clearance is more appropriately measured for hepatic clearance prediction. Eventually, human clearance predictions of potential drug candidates can be generated with the Extended Clearance Model method.

For the other ECCS class 1a/2/3a/4 compounds, suspended hepatocytes could be used effectively for metabolic clearance optimization and initial clearance estimations during lead optimization. It is recommended that a long-term culture system, such as HepatoPac, is used for the human clearance prediction of potential drug candidates to obtain the best currently possible predictions. A strategy for the selection of the in vitro tools for metabolic clearance evaluation is proposed here, especially taking into consideration cost effectiveness in drug development (Fig. 4B). For compounds with CLint,h ≤3 μl/min per 10^6 cells in suspended hepatocytes (low clearance), reassessment of CLint,h

using HepatoPac should be considered to achieve a reasonable IVIVE. With 3 < CLint,h ≤ 30 μl/min per 10^6 cells (moderate clearance), CLint,h in suspended hepatocytes can be used for the clearance prediction (Docci et al., 2019). However, it is noted that a >3-fold underestimation of upscaled CLint,h,u (milliliters per minute per kilogram) in hepatocyte suspension relative to the reference in vivo CLint,h,u is likely when CLint,h is ≤10 μl/min per 10^6 (Fig. 3A; Table 2). Based on an internal assessment (data not shown), human liver microsomes generally provide accurate and precise in vitro metabolic turnover with CLint,h ≥30 μl/min per 10^6 cells (high clearance).

In conclusion, low passive permeability can be used to identify molecules whose in vivo clearance is driven by active uptake, such as carboxylic acids. The HepatoPac system suitable for the assessment of metabolic turnover has limited predictability of uptake, likely due to measurability challenges (small amount of drug material taken up with cellular mass of the system). Therefore, measurement of uptake clearance during a short-term incubation using suspended hepatocytes is proposed. Nevertheless, the in vivo hepatic clearance would not be captured because of a lack of biliary excretion in such in vitro systems. Clear knowledge of system limitations enables project teams to anticipate when IVIVE methods will result in misprediction of hepatic clearance and select the most relevant test systems for compound optimization. The validation and approach presented here provide more confidence in mechanistic human PK prediction with modeling and simulation support.

Authorship Contributions

Participated in research designs: Umehara, Cantrill, Wittwer, Fowler, Ullah.

Conducted experiments: Di Lenarda, Klammers, Ekiciler.

Performed data analysis: Umehara, Cantrill, Wittwer, Di Lenarda, Klammers, Ullah.

Wrote or contributed to the writing of the manuscript: Umehara, Cantrill, Wittwer, Parrott, Fowler, Ullah.

References

Anderle P, Niederer E, Rubas W, Hilgendorf C, Spahn-Langguth H, Wunderli-Allenspach H, Merkle HP, and Langguth P (1998) P-Glycoprotein (P-gp) mediated efflux in Caco-2 cell monolayers: the influence of culturing conditions and drug exposure on P-gp expression levels. *J Pharm Sci* **87**:757–762.

Baldock GA, Brodie RR, Chasseaud LF, and Taylor T (1990) Determination of benzydamine and its N-oxide in biological fluids by high-performance liquid chromatography. *J Chromatogr A* **529**:113–123.

Bednarczyk D and Sanghvi MV (2020) The impact of assay recovery on the apparent permeability, a function of lysosomal trapping. *Xenobiotica* **50**:753–760.

Bohnert T, Patel A, Templeton I, Chen Y, Lu C, Lai G, Leung L, Tse S, Einolf HJ, Wang YH, et al.; International Consortium for Innovation and Quality in Pharmaceutical Development (IQ) Victim Drug-Drug Interactions Working Group (2016) Evaluation of a new molecular entity as a victim of metabolic drug-drug interactions-an industry perspective. *Drug Metab Dispos* **44**: 1399–1423.

Bullingham RE, Nicholls AJ, and Kamm BR (1998) Clinical pharmacokinetics of mycophenolate mofetil. *Clin Pharmacokinet* **34**:429–455.

Caldwell JH and Cline CT (1976) Biliary excretion of digoxin in man. *Clin Pharmacol Ther* **19**: 410–415.

Camenisch G and Umehara K (2012) Predicting human hepatic clearance from in vitro drug metabolism and transport data: a scientific and pharmaceutical perspective for assessing drug-drug interactions. *Biopharm Drug Dispos* **33**:179–194.

Chan TS, Yu H, Moore A, Khetani SR, and Tweedie D (2019) Meeting the challenge of predicting hepatic clearance of compounds slowly metabolized by cytochrome P450 using a novel hepatocyte model, HepatoPac. *Drug Metab Dispos* **47**:58–66.

Docci L, Parrott N, Krähenbühl S, and Fowler S (2019) Application of new cellular and micro-physiological systems to drug metabolism optimization and their positioning respective to in silico tools. *SLAS Discov* **24**:523–536.

Echizen H and Ishizaki T (1991) Clinical pharmacokinetics of famotidine. *Clin Pharmacokinet* **21**: 178–194.

Fredlund L, Winiwarter S, and Hilgendorf C (2017) In vitro intrinsic permeability: a transporter-independent measure of caco-2 cell permeability in drug design and development. *Mol Pharm* **14**:1601–1609.

Fujino H, Saito T, Tsunenari Y, Kojima J, and Sakaeda T (2004) Metabolic properties of the acid and lactone forms of HMG-CoA reductase inhibitors. *Xenobiotica* 34:961–971.

Giessmann T, May K, Modess C, Wegner D, Hecker U, Zschiesche M, Dazert P, Grube M, Schroeder E, Warzok R, et al. (2004) Carbamazepine regulates intestinal P-glycoprotein and multidrug resistance protein MRP2 and influences disposition of talinolol in humans. *Clin Pharmacol Ther* 76:192–200.

Hultman Ia, Vedin C, Abrahamsson A, Winiwarter S, and Darnell M (2016) Use of HμREL human coculture system for prediction of intrinsic clearance and metabolite formation for slowly metabolized compounds. *Mol Pharm* 13:2796–2807.

Iwatsubo T, Hirota N, Ooie T, Suzuki H, Shimada N, Chiba K, Ishizaki T, Green CE, Tyson CA, and Sugiyama Y (1997) Prediction of in vivo drug metabolism in the human liver from in vitro metabolism data. *Pharmacol Ther* 73:147–171.

Johnson TN, Tucker GT, Tanner MS, and Rostami-Hodjegan A (2005) Changes in liver volume from birth to adulthood: a meta-analysis. *Liver Transpl* 11:1481–1493.

Keskitalo JE, Pasanen MK, Neuvonen PJ, and Niemi M (2009) Different effects of the ABCG2 c.421C>A SNP on the pharmacokinetics of fluvastatin, pravastatin and simvastatin. *Pharmacogenomics* 10:1617–1624.

Khetani SR and Bhatia SN (2008) Microscale culture of human liver cells for drug development. *Nat Biotechnol* 26:120–126.

Kim JH, Choi WG, Lee S, and Lee HS (2017) Revisiting the metabolism and bioactivation of ketoconazole in human and mouse using liquid chromatography-mass spectrometry-based metabolomics. *Int J Mol Sci* 18:621.

Kratochwil NA, Meille C, Fowler S, Klammers F, Ekiciler A, Molitor B, Simon S, Walter I, McGinnis C, Walther J, et al. (2017) Metabolic profiling of human long-term liver models and hepatic clearance predictions from in vitro data using nonlinear mixed-effects modeling. *AAPS J* 19:534–550.

Kratochwil NA, Triyatni M, Mueller MB, Klammers F, Leonard B, Turley D, Schmaler J, Ekiciler A, Molitor B, Walter I, et al. (2018) Simultaneous assessment of clearance, metabolism, induction, and drug-drug interaction potential using a long-term in vitro liver model for a novel hepatitis B virus inhibitor. *J Pharmacol Exp Ther* 365:237–248.

Kunze A, Huwyler J, Camenisch G, and Poller B (2014) Prediction of organic anion-transporting polypeptide 1B1- and 1B3-mediated hepatic uptake of statins based on transporter protein expression and activity data. *Drug Metab Dispos* 42:1514–1521.

Kusuhara H and Sugiyama Y (2010) Pharmacokinetic modeling of the hepatobiliary transport mediated by cooperation of uptake and efflux transporters. *Drug Metab Rev* 42:539–550.

Lee JB, Zgair A, Taha DA, Zang X, Kagan L, Kim TH, Kim MG, Yun HY, Fischer PM, and Gershkovich P (2017) Quantitative analysis of lab-to-lab variability in Caco-2 permeability assays. *Eur J Pharm Biopharm* 114:38–42.

Li J, Volpe DA, Wang Y, Zhang W, Bode C, Owen A, and Hidalgo IJ (2011) Use of transporter knockdown Caco-2 cells to investigate the in vitro efflux of statin drugs. *Drug Metab Dispos* 39:1196–1202.

Lin C and Khetani SR (2016) Advances in engineered liver models for investigating drug-induced liver injury. *BioMed Res Int* 2016:1829148.

Lombardo F, Obach RS, Shalaeva MY, and Gao F (2004) Prediction of human volume of distribution values for neutral and basic drugs. 2. Extended data set and leave-class-out statistics. *J Med Chem* 47:1242–1250.

Maeda K, Ikeda Y, Fujita T, Yoshida K, Azuma Y, Haruyama Y, Yamane N, Kumagai Y, and Sugiyama Y (2011) Identification of the rate-determining process in the hepatic clearance of atorvastatin in a clinical cassette microdosing study. *Clin Pharmacol Ther* 90:575–581.

Malmborg J and Ploeger BA (2013) Predicting human exposure of active drug after oral prodrug administration, using a joined in vitro/in silico-in vivo extrapolation and physiologically-based pharmacokinetic modeling approach. *J Pharmacol Toxicol Methods* 67:203–213.

Mathialagan S, Piotrowski MA, Tess DA, Feng B, Litchfield J, and Varma MV (2017) Quantitative prediction of human renal clearance and drug-drug interactions of organic anion transporter substrates using in vitro transport data: a relative activity factor approach. *Drug Metab Dispos* 45:409–417.

Mathijssen RH, van Alphen RJ, Verweij J, Loos WJ, Nooter K, Stoter G, and Sparreboom A (2001) Clinical pharmacokinetics and metabolism of irinotecan (CPT-11). *Clin Cancer Res* 7:2182–2194.

McGinnity DF, Soars MG, Urbanowicz RA, and Riley RJ (2004) Evaluation of fresh and cryopreserved hepatocytes as in vitro drug metabolism tools for the prediction of metabolic clearance. *Drug Metab Dispos* 32:1247–1253.

Murgasova R (2019) Further assessment of the relay hepatocyte assay for determination of intrinsic clearance of slowly metabolised compounds using radioactivity monitoring and LC-MS methods. *Eur J Drug Metab Pharmacokinet* 44:817–826.

Patel KS, Stephany BR, Barnes JF, Bauer SR, and Spinner ML (2017) Renal transplant acute rejection with lower mycophenolate mofetil dosing and proton pump inhibitors or histamine-2 receptor antagonists. *Pharmacotherapy* 37:1507–1515.

Picard N, Ratanasavanh D, Prémaud A, Le Meur Y, and Marquet P (2005) Identification of the UDP-glucuronosyltransferase isoforms involved in mycophenolic acid phase II metabolism. *Drug Metab Dispos* 33:139–146.

Poirier A, Cascais AC, Bader U, Portmann R, Brun ME, Walter I, Hillebrecht A, Ullah M, and Funk C (2014) Calibration of in vitro multidrug resistance protein 1 substrate and inhibition assays as a basis to support the prediction of clinically relevant interactions in vivo. *Drug Metab Dispos* 42:1411–1422.

Polasek TM, Doogue MP, and Miners JO (2011) Metabolic activation of clopidogrel: in vitro data provide conflicting evidence for the contributions of CYP2C19 and PON1. *Ther Adv Drug Saf* 2:253–261.

Poulin P and Theil FP (2002) Prediction of pharmacokinetics prior to in vivo studies. 1. Mechanism-based prediction of volume of distribution. *J Pharm Sci* 91:129–156.

Reddy VP, Jones BC, Colclough N, Srivastava A, Wilson J, and Li D (2018) An investigation into the prediction of the plasma concentration-time profile and its interindividual variability for a range of flavin-containing monooxygenase substrates using a physiologically based pharmacokinetic modeling approach. *Drug Metab Dispos* 46:1259–1267.

Riede J, Umehara KI, Schweigler P, Huth F, Schiller H, Camenisch G, and Poller B (2019) Examining P-gp efflux kinetics guided by the BDDCS - rational selection of in vitro assay designs and mathematical models. *Eur J Pharm Sci* 132:132–141.

Schuhmacher J, Bühner K, and Witt-Laido A (2000) Determination of the free fraction and relative free fraction of drugs strongly bound to plasma proteins. *J Pharm Sci* 89:1008–1021.

Scotcher D, Jones C, Rostami-Hodjegan A, and Galetin A (2016) Novel minimal physiologically-based model for the prediction of passive tubular reabsorption and renal excretion clearance. *Eur J Pharm Sci* 94:59–71.

Shibata Y, Takahashi H, Chiba M, and Ishii Y (2002) Prediction of hepatic clearance and availability by cryopreserved human hepatocytes: an application of serum incubation method. *Drug Metab Dispos* 30:892–896.

Shimizu M, Fuse K, Okudaira K, Nishigaki R, Maeda K, Kusuhara H, and Sugiyama Y (2005) Contribution of OATP (organic anion-transporting polypeptide) family transporters to the hepatic uptake of fexofenadine in humans. *Drug Metab Dispos* 33:1477–1481.

Somogyi A and Gugler R (1983) Clinical pharmacokinetics of cimetidine. *Clin Pharmacokinet* 8:463–495.

Swift B, Pfeifer ND, and Brouwer KL (2010) Sandwich-cultured hepatocytes: an in vitro model to evaluate hepatobiliary transporter-based drug interactions and hepatotoxicity. *Drug Metab Rev* 42:446–471.

Thiel C, Schneckener S, Krauss M, Ghallab A, Hofmann U, Kanacher T, Zellmer S, Gebhardt R, Hengstler JG, and Kuepfer L (2015) A systematic evaluation of the use of physiologically based pharmacokinetic modeling for cross-species extrapolation. *J Pharm Sci* 104:191–206.

Toshimoto K, Tomaru A, Hosokawa M, and Sugiyama Y (2017) Virtual clinical studies to examine the probability distribution of the AUC at target tissues using physiologically-based pharmacokinetic modeling: application to analyses of the effect of genetic polymorphism of enzymes and transporters on irinotecan induced side effects. *Pharm Res* 34:1584–1600.

Tse FL, Nickerson DF, and Yardley WS (1993) Binding of fluvastatin to blood cells and plasma proteins. *J Pharm Sci* 82:942–947.

Umehara K and Camenisch G (2012) Novel in vitro-in vivo extrapolation (IVIVE) method to predict hepatic organ clearance in rat. *Pharm Res* 29:603–617.

US Food and Drug Administration. (2020) Drugs@FDA: FDA approved drug products.: drug interaction studies - study design, data analysis, implications for dosing, and labeling recommendations. Available at: https://www.accessdata.fda.gov/scripts/cder/daf/

Varma MV, El-Kattan AF, Feng B, Steyn SJ, Maurer TS, Scott DO, Rodrigues AD, and Tremaine LM (2017) Extended Clearance Classification System (ECCS) informed approach for evaluating investigational drugs as substrates of drug transporters. *Clin Pharmacol Ther* 102:33–36.

Varma MV, Steyn SJ, Allerton C, and El-Kattan AF (2015) Predicting clearance mechanism in drug discovery: Extended Clearance Classification System (ECCS). *Pharm Res* 32:3785–3802.

Waldmeier F, Flesch G, Müller P, Winkler T, Kriemler HP, Bühlmayer P, and De Gasparo M (1997) Pharmacokinetics, disposition and biotransformation of [14C]-radiolabelled valsartan in healthy male volunteers after a single oral dose. *Xenobiotica* 27:59–71.

Watanabe T, Kusuhara H, Maeda K, Kanamaru H, Saito Y, Hu Z, and Sugiyama Y (2010) Investigation of the rate-determining process in the hepatic elimination of HMG-CoA reductase inhibitors in rats and humans. *Drug Metab Dispos* 38:215–222.

Ye M, Nagar S, and Korzekwa K (2016) A physiologically based pharmacokinetic model to predict the pharmacokinetics of highly protein-bound drugs and the impact of errors in plasma protein binding. *Biopharm Drug Dispos* 37:123–141.

Zhang S and Morris ME (2003) Effect of the flavonoids biochanin A and silymarin on the P-glycoprotein-mediated transport of digoxin and vinblastine in human intestinal Caco-2 cells. *Pharm Res* 20:1184–1191.

Address correspondence to: Dr. Kenichi Umehara, Investigative Safety, In Vitro Pharmacokinetics (PK) and Drug-Drug Interaction (DDI) Section, Roche Pharmaceutical Research and Early Development, Grenzacherstrasse 124, CH-4070 Basel, Switzerland. E-mail: kenichi.umehara@roche.com